

HOSTED BY



Gulf Organisation for Research and Development

International Journal of Sustainable Built Environment

ScienceDirect
www.sciencedirect.com

Original Article/Research

Indoor heat stress and cooling energy comparison between green roof (GR) and non-green roof (n-GR) by simulations for labor intensive factories in the tropics

Sajal Chowdhury^{a,b,*}, Yasuhiro Hamada^b, Khandaker Shabbir Ahmed^c^a Department of Architecture, Chittagong University of Engineering & Technology, Chittagong 4349, Bangladesh^b Laboratory of Environmental Ergonomics, Research Group of Planning and Performances for Built Environment, Division of Human Environmental Systems, Faculty of Engineering, Hokkaido University, Kita-ku, Sapporo, Hokkaido 060-8628, Japan^c Department of Architecture, Bangladesh University of Engineering & Technology, Dhaka 1000, Bangladesh

Received 26 April 2017; accepted 17 September 2017

Abstract

This study is based on labor intensive factory, located in Dhaka, Bangladesh which was adversely impacted due to extreme hot conditions. The analysis started with the implementation of green roof (GR) as one of the passive design strategies to reduce indoor heat stress. Impact of indoor heat stress indicated by wet bulb globe temperature (WBGT) and prediction of heat strain (PHS) model for green roof have been evaluated through numerical studies and indoor environmental data of local factory was measured by portable weather station. A factory energy model (by Energyplus and Open Studio) based on one of the surveyed factory's production space including different activity zones and lab test material's properties was developed and different roof variables were evaluated. The result indicated that GR has significant contributions on indoor heat stress reduction and substrate indoor temperature decreases (2.5–3.5 °C) with increasing vegetal coverage. It has been also examined the ratio of indoor temperature fluctuation and relatively higher standard deviation (SD) observed for non-green roof (n-GR) condition. For summer, it was also quantified that indoor WBGT and PHS criteria for the workers became 2–2.5 times lower from the high risk level due to the effectiveness of GR.

© 2017 The Gulf Organisation for Research and Development. Production and hosting by Elsevier B.V. All rights reserved.

Keywords: Indoor heat stress; Green roof; Non-green roof; Tropical climate; Production space

1. Introduction

In Bangladesh, the labor intensive factories' [like garments factories] indoor thermal environment (AT & RH)

has been criticized over the years for its excessive hot environment in the production spaces (Nahar et al., 2010; Chowdhury et al., 2015). According to the Bangladesh Garments Manufacturers and Exporters Association (BGMEA) (2015), more than 4 million workers (mostly women) are working day long in approximately five thousand and six hundred garments factories in Bangladesh. Since the field monitoring, it has been detected that indoor thermal environment of many purpose built factories in

* Corresponding author at: Department of Architecture, Chittagong University of Engineering & Technology, Chittagong 4349, Bangladesh.
E-mail addresses: sajal_c@cuet.ac.bd, sajal_c@yahoo.com (S. Chowdhury).

Peer review under responsibility of The Gulf Organisation for Research and Development.

Nomenclature

a	area (m ²)	SD	standard deviation
AMY	actual meteorological year	SR	solar radiation (W/m ²)
AT	air temperature (°C)	t	temperature (°C)
C _p	specific heat (J kg ⁻¹ K ⁻¹)	t _{cr}	core temperature (°C)
d	thickness (m)	t _{sk}	skin temperature (°C)
EPW	energy plus weather data	T _w	Natural WBT (Wet Bulb Temperature)
GR	green roof	T _g	Globe thermometer temperature
h	height (m)	T _{pwb}	Psychrometric wet bulb temperature
k	conductivity (W m ⁻¹ K ⁻¹)	T _a	Air temperature
LAI	leaf area index	ΔT	temperature difference (°C)
m	mass (kg)	TMY	typical meteorological year
n-GR	non green roof	V	volume (m ³)
Q	amount of heat (J)	w	depth (m)
R	thermal resistance (m ² kW ⁻¹)	WS	wind speed (m s ⁻¹)
RCC	reinforce concrete	x	length (m)
RH (%)	relative humidity (%)	ρ	true density (kg/m ³)
S	specific heat of metal disc (J kg ⁻¹ K ⁻¹)		

Bangladesh becomes excessively higher than the comfortable range (25.5–28 °C) (Table 1) Nahar et al., 2010 and at the individual worker level, increased body temperatures stimulate the incapability to balance the heat flows from the human body by the thermoregulation system (Buchin et al., 2015a). Therefore Skin Temperature (t_{sk}) and Core Temperature (t_{cr}) Bernard and Mark Hanna, 1988; Malchaire, 2006 of the workers have been extremely affected by hot indoor temperature leading to serious health hazardous (heat rash, heat cramps, heat exhaustion, heat stroke et al.) for the factory workers and also reduce the productivity (Chowdhury et al., 2017). Various passive design strategies could be an effective way to reduce indoor heat stress now-a-days (Chowdhury and Alam, 2011; Fiorito, 2014; Yang et al., 2015; Naz, 2008). This study attempts to explore the indoor heat stress evaluation (WBGT and PHS) of workers for local labor intensive factories with the implementation of GR as one of the passive design strategies to reduce indoor heat stress in comparison with non- green roof (n-GR) condition by parametric studies.

2. Research methodology

The research methodology (Fig. 1) has been segmented into the following measures:

- To obtain the basic statistics of the indoor thermal performance level of existing production spaces without GR, with special reference to Dhaka, a predetermined interval field monitoring by the data logger (HOBO Weather Station Pro 30) (Chowdhury et al., 2015) has been conducted to measure AT, RH and WS.

- To determine the accuracy of simulation studies, properties of local available construction materials have been ascertained from laboratory experiments (Table 2) and applied in the parametric studies using building energy simulation engine, Energy plus Version 8.1.0 (Crawley et al., 2001) with 'Open studio Plug-in 1.3.0 integrated with Google Sketch-Up 8 (Al-Zubaydi, 2013). It may be noted here that in this study, the thermal properties (Conductivity, Specific heat, Density, Resistance) of local available construction materials have been identified using Lee's and Charlton's apparatus at the material testing laboratory of the Dept. of Materials & Metallurgical Engineering, (BUET) in Bangladesh (Chowdhury et al., 2015).
- After accompanying environmental monitoring, a three dimensional energy model has been conducted by simulation engine 'Energy plus' with 'Open studio Plug-in' (Fig. 2). For accuracy, simulated factory production space environment should be similar as the surveyed factory production space according to the main functions and production workflow (sewing activity) Chowdhury et al., 2017, so that it could easily associate the simulation results between the existing (n-GR) and predicted (GR) conditions.
- For the validation and comparison of the analysis, the resulting average indoor comfort range (Table 1) (Chowdhury et al., 2015; Shabbir Ahmed, 2003) was set up to be an effective condition from the literature survey.
- A series of simulation studies have been evaluated for the prediction of WBGT and PHS according to their internationally established criteria and formula (Bernard and Mark Hanna, 1988; (Parsons, 2006;

Table 1

Field and recommended thermal comfort data for simulations.

From field monitoring					Comfort criteria		
Avg. Outdoor Temperature (°C)	Maximum Surface Temp (°C)	Minimum Surface Temperature (°C)	Avg. Indoor Temperature (°C)	Approx. Difference from Comfort Range (°C)	Comfort Temperature Range (°C)	Humidity (%)	Mean Air Speed (m s ⁻¹)
(28 ~ 35)	(34.44 ~ 42.30)	(24 ~ 29)	(30 ~ 32)	(6.5 ~ 14.3)	Comfort (25.5 ~ 28) Moderate (28 ~ 32)	<65	0.25 ~ 0.5

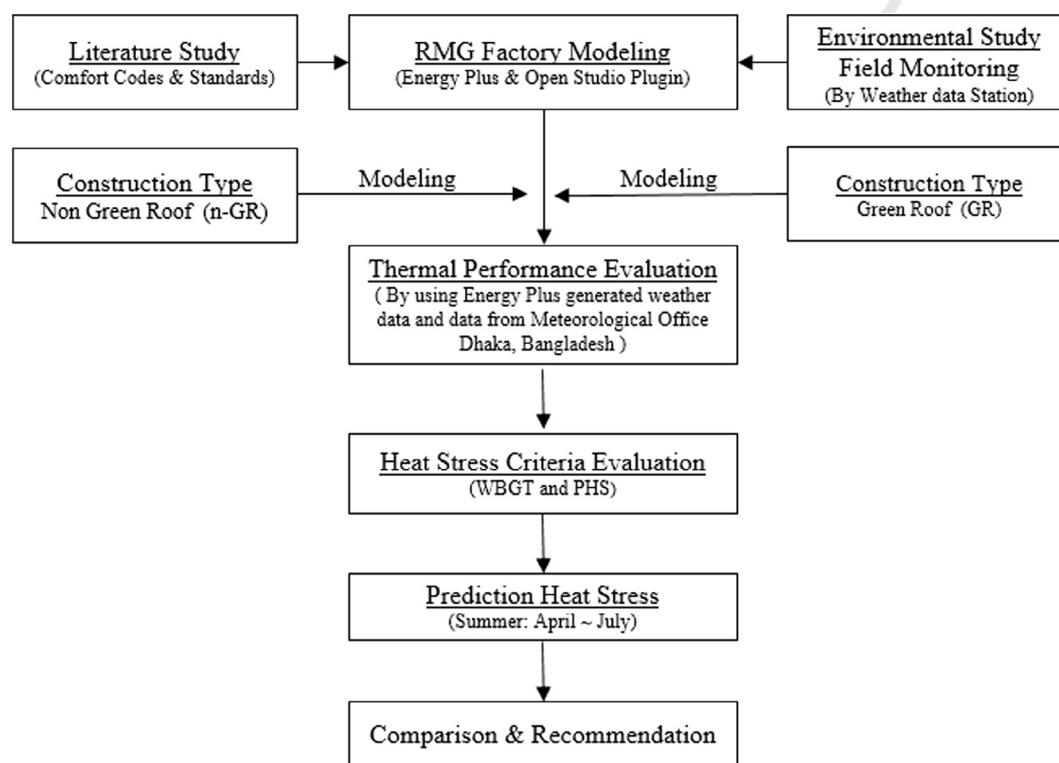


Fig. 1. Structure of the research work.

Lemke and Kjellstrom, 2012; Moran et al., 2001; Ergonomics of the thermal environment, 2004; Parsons, 2009) under the local climate consideration.

3. Parametric setup and numerical scheme

3.1. Selection of the production space

The workflow framework of the simulated labor intensive factory building's production space should be similar as one of the surveyed factory's production spaces (sewing section with minimum 5 production lines) which were conducted from Nov. 2009 to March 2010 and different periods in 2013–14 and guided by BGMEA, Green Architecture Cell (GrACe) (BUET) and Deutsche Gesellschaft für Internationale Zusammenarbeit (GIZ) in the Dhaka region, Bangladesh (Chowdhury et al., 2015; Bangladesh Garments Manufactures and Exporters Association

(BGMEA), 2015). It may be noted here that in this studies only indoor factory workflow and environment have been considered for modeling purpose and outdoor measured environmental factors (AT, WS and RH) considered for the simulation [Table 1].

3.2. Local climate characterization

According to the tropical climatic consideration, there are three different seasons in Bangladesh (Chowdhury et al., 2015; Chowdhury et al., 2017; Shabbir Ahmed, 2003): a hot, humid summer; a cool, rainy monsoon season; and a cool, dry winter. In this study, for the effective heat stress comparison, whole simulations have been evaluated for the months of April–July (summer). In general, summer temperatures (April–July) range remain between 28 and 40 °C. The TMY data (outdoor design parameters and hourly weather data), developed by the Energy Plus, Dhaka 419230 SWERA, has been commonly used in this

Table 2

Thermal properties of local available construction materials (lab measurement data range).

Name	Brick	Tiles	RCC	Plaster	Glass
Roughness	Smooth	Smooth	Medium smooth	Medium Rough	
Thickness (m)	0.254	0.0063	0.127/0.254	0.0063	0.003
Conductivity (W/m-k)	0.55–1.34	1.12	1.34	0.43	0.9
Density (kg/m ³)	1200–1789	1763	2487	2374	Front Solar Reflectance = 0.075
Specific Heat (J/kg-K)	1150–1450	1200–1350	670–850	650–750	Back Solar Reflectance = 0.075
Thermal Absorptance	0.9	0.9	0.9	0.9	Infrared transmittance = 0
Solar Absorptance	0.7	0.7	0.7	0.7	Solar transmittance = 0.8
Visible Absorptance	0.7	0.7	0.7	0.7	Visible transmittance = 0.8

Exterior n-GR roof construction

RCC 1:2:4 ratio (Cement: Sand: Aggregate)

Tiles: 12.7 mm

Bitumin: 3 mm

Both side plaster: 30 mm

RCC thickness: 150 mm

Local bricks

Classes: (1st, 2nd and 3rd)

Brick thickness, d = 254 mm

Plaster, d = 6.35 mm

Window height, h = 1.52 m

Sill height, h = 0.76 m.

Opening systems = sliding

Aluminum frame with clear float glass

opening area = 50% of the total opening area

RCC 1:2:4 ratio

(Cement: Sand: Aggregate)

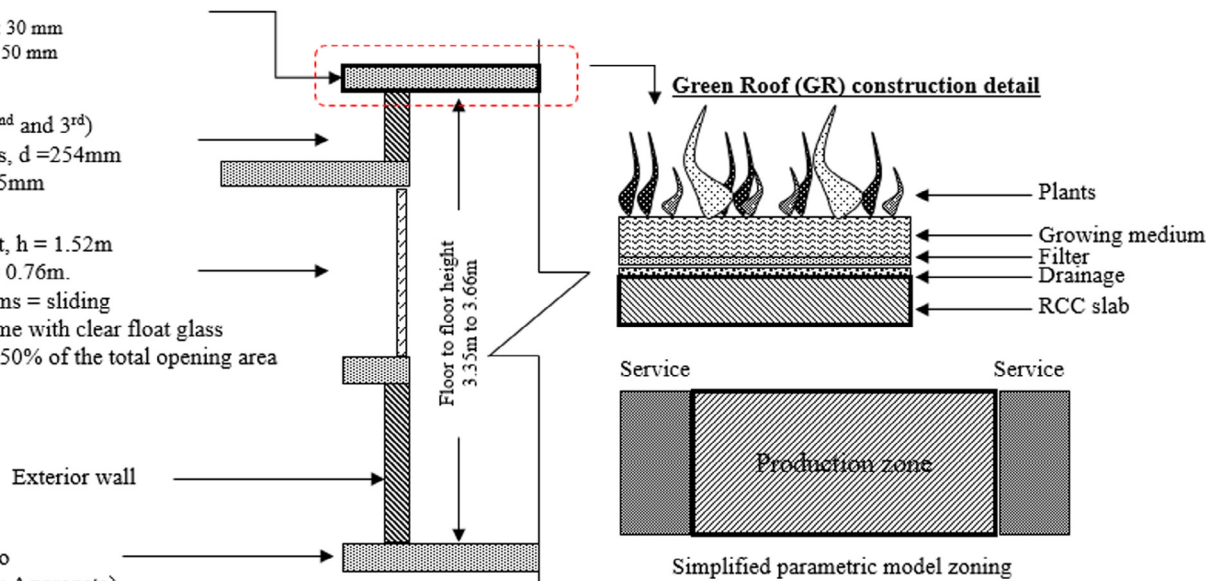


Fig. 2. Floor plan and green roof section detail of simulated RMG production zone.

parametric study and for more accuracy a comparison has been conducted with AMY generated data from Meteorological Office Dhaka, Bangladesh (Fig. 3) (Hygh et al., 2012; Wittwer et al., 2004; EnergyPlus and U.S. Department of Energy, 2015; Meteorological Department and IDB Bhaban, 2015).

3.3. Construction types

Local construction types (GR and n-GR) were evaluated in this study (Fig. 3). Two basic models of the factory production spaces (GR and n-GR) were simulated in similar indoor settings and indoor thermal performances were evaluated using the Energy plus and Open studio Plug-in (Fig. 2). The first model has been considered as single storied RMG production space including functional services with a conventional roof constructed from these layers: external and internal air film, 3 mm bitumen, 30 mm outer plaster and tiles, 150 mm reinforced concrete, and 12.5 mm internal plaster. The other model has the same building conditions but its roof has been covered with a (150–180)

mm soil layer and green trees (height 0.2–0.25 m) with LAI 2.7 (Table 3). It should be noted here that basically two main types of green roofs are commonly applied: intensive and extensive. In this analysis, extensive type (about 5–20 cm) green roof has been analyzed which was comprised of several layers laid in sequence: root barrier, drainage and storage layer, filter layer, soil (substrate), and vegetation. The external wall, window, roof structure and materials are detailed in Fig. 2. Simulated results for each construction type have been analyzed in terms of statistical meaning (Ergonomics of the thermal environment, 2004; Parsons, 2009).

The entire simulation configuration database is given in Table 4.

4. Result analysis and discussion

From the comparison of AMY, TMY and EPW, it has been observed that physical measurement of indoor RH was fluctuated not more than $\pm 5\text{--}7\%$ from the predicted results (Fig. 3) which appeared as an acceptable error.

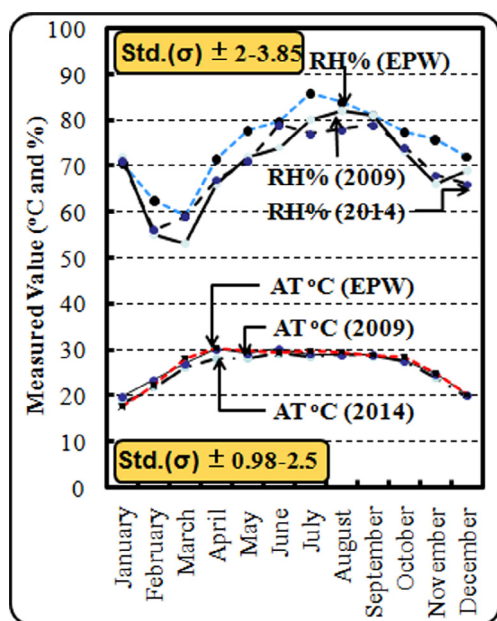


Fig. 3. Comparison outdoor AT and RH (measured and simulated).

On the other hand Fig. 3 also indicates that the difference between measured and simulated AT was not more than $\pm 1-2^{\circ}\text{C}$ ($30-32^{\circ}\text{C}$ avg.) for the month of April–July and has been observed almost same in all conditions. In this analysis the “conduction transfer function” heat balance algorithm has been applied and the “simple sky diffuse model” has been adopted.

4.1. Indoor AT and RH prediction calculation

The comparative illustration of the indoor AT and RH (variations) with GR and n-GR condition for the test production space during the indicative operational days have

been shown in Fig. 4(a)–(b) and deviation in Fig. 5 respectively. It was found that indoor AT and RH for test room presented very similar trend of fluctuation (Fig. 5), while the simulated space had a bit higher average and maximum range of temperature difference than before ($28.90-35.72^{\circ}\text{C}$). Compared to the production space with n-GR, the test production space with GR remained the lowest indoor AT ($2.5-3.5^{\circ}\text{C}$ lower than n-GR) which was around $27.5-28.5^{\circ}\text{C}$ in average, while the n-GR represents the highest indoor temperature which was around $30.6-32.8^{\circ}\text{C}$ in average with the condition of natural ventilation. On the other hand, from this analysis, it was also observed that for GR, indoor RH respectively changed and became higher with respect to outdoor RH and having n-GR and varied from one to another construction type (n-GR to GR) was examined from 8% to 12% respectively Fig. 4(b).

4.2. Indoor WBGT prediction calculation

The whole calculations have been formulated according to the ISO 7243 and the OSHA Technical Manual, Section III, Chapter IV, (Heat stress) (Bernard and Mark Hanna, 1988; Malchaire, 2006; Parsons, 2006; Lemke and Kjellstrom, 2012; Moran et al., 2001; Ergonomics of the thermal environment, 2004). Here, WBGT is one of the most widely used heat stress indices which was derived from a series of research around 1920 that became the established method used to evaluate heat stress (Parsons, 2006; Lemke and Kjellstrom, 2012; Moran et al., 2001). The index combined AT, RH, SR and WS into a single value which could be used for the assessments (Parsons, 2006). In this research the following established criteria has been applied for the prediction of indoor WBGT between n-GR and GR construction type.

Table 3
Properties of Green Roof (GR) Model.

Name	Unit	Eco Roof Model
Height of plants	m	0.2–0.25
Leaf Area Index ($LAI = \text{leaf area/ground area, m}^2/\text{m}^2$)	dimensionless	2.7
Leaf Reflectivity	dimensionless	0.2
Leaf Emissivity		0.95
Minimum Stomatal Resistance	s/m	180
Soil Layer Name		Green Roof Soil
Roughness		Medium Smooth
Thickness	m	0.36
Conductivity of Dry Soil	W/m-k	1.5
Density of Dry Soil	kg/m ³	641
Specific Heat of dry Soil	J/kg-K	800
Thermal Absorptance		0.9
Solar Absorptance		0.8
Visible Absorptance		0.7
Saturation Volumetric Moisture Content of Soil Layer		0.4
Residual Volumetric Moisture Content of Soil Layer		0.01
Initial Volumetric Moisture Content of Soil Layer		0.2
Moisture Diffusion Calculation Method		Advanced

(Source: Sailor et al., January 2007).

Table 4
Factory parameters for Energy Plus simulation.

Parameters	Specifications
Location	Within greater Dhaka region, Bangladesh
Geographical Location:	
i) Longitude	90.25° (North)
ii) Latitude	23.95° (East)
Time Zone	+6 GMT
Simulation period	April–July 2014 (Condition: Summer with high Temperature & Humidity)
Sky Model	Clear sky
Calculation option	Standard
Units of Dimensions (Length, areas, etc.)	Metric (SI) (m, cm, etc.)
Units of Photometric Dimension	European (SI) (lux, cd/m ² , etc.)
Elevation	9 m
Orientation	Front Elevation facing South
Plan Shape	Rectangular
Total number of floor	1
Simulated floor	Production Zone (Sewing)
Floor to Floor Height	3.5 m (7.0 m for the two floors)
Floor Area	330 m ²
Floor Dimension	13.5 m × 24.5 m
Window Area	15% of the gross wall area, Uniformly distributed
Solar Absorbance (for exterior surfaces)	0.55 for external walls (Light color) 0.35 for the roof (light color)
Occupancy Density	150 Nos./floor
Lighting level	350 lux (max) for sewing
Electric equipment	220 Watts/Person
Glazing	Single panel of glass with aluminum frame (refl. 0.92)
Construction Type	ASHRAE 90.1 non Res.
Natural Ventilation	Simple (Operable simple window)(One Array)
Zone Ventilation Flow rate	0.25–4.0 (Flow/Hour) (Effective Air Leakage Area = 25 m ² avg.)
Room Air Distribution Model	General cross ventilation and exhaust type (0.25–4.0: Air Changes/Hour)
Ventilation Control Mode	Temperature (off/on)
Design Flow Rate	0.25–4.0 (Air Changes/Hour)
Air gap thermal resistance	0.13–0.50 m ² kw ⁻¹
Design Flow Rate Calculation Method	Air Changes/Hour
Leakage Component Name	Surface Object
Factory construction	Roof: Plaster (1:5)+ RCC (1:2:4)+ Plaster (1:5) Floor: Plaster (1:5)+ RCC (1:2:4)+ Plaster (1:5) Wall: Brick wall, Plaster (1:5)+ Brick + Plaster (1:5)+ air gap + Plaster (1:5)+ Brick + Plaster (1:5) (construction pattern has been changed alternatively) Opening: Clear 6 mm (sliding) Shading: (1:5)+ RCC (1:2:4)+ Plaster (1:5)
Mechanical ventilation	None
Output variable	AT (°C), MRT (°C), OP (°C), RH (%)
Schedule Type Limit	Fraction/ Continuous
Fraction Radiant	0.3–0.4
Output Variable Dictionary	Regular
Output Schedule	Hourly
Heat balance algorithm	Conduction transfer function

$$WBGT = 0.7T_w + 0.3T_g = 0.7T_w + 0.3T_a \quad (1)$$

[For, indoors, or when solar radiation is negligible Moran et al., 2001; Ergonomics of the thermal environment, 2004; considering $WS \geq 3 \text{ ms}^{-1}$, $T_w = T_{pwb}$; $T_g = T_a$]

From the analysis (Figs. 6 and 7), it has been observed that for the GR construction type, indoor WBGT remained 2–2.5 °C in lower condition for the month of April–July than n-GR construction type. For GR, the maximum indoor WBGT was observed in summer (June–

July) with an average of 28 °C and the lower level was found about 26.5–27 °C in the month of April, whereas, the higher WBGT was found up to 30 °C in July and lower was 29 °C in April for the n-GR construction type. Meanwhile, the SD of WBGT between n-GR and GR construction has been analyzed almost ± 2 °C (avg.). From the numerical analysis (Fig. 6), it was also observed that from April to July WBGT predicted a very high risk condition almost 22–25% for n-GR, whereas, for GR construction, there was not a very high risk condition; meanwhile, the lower (comfortable) condition increased almost two times

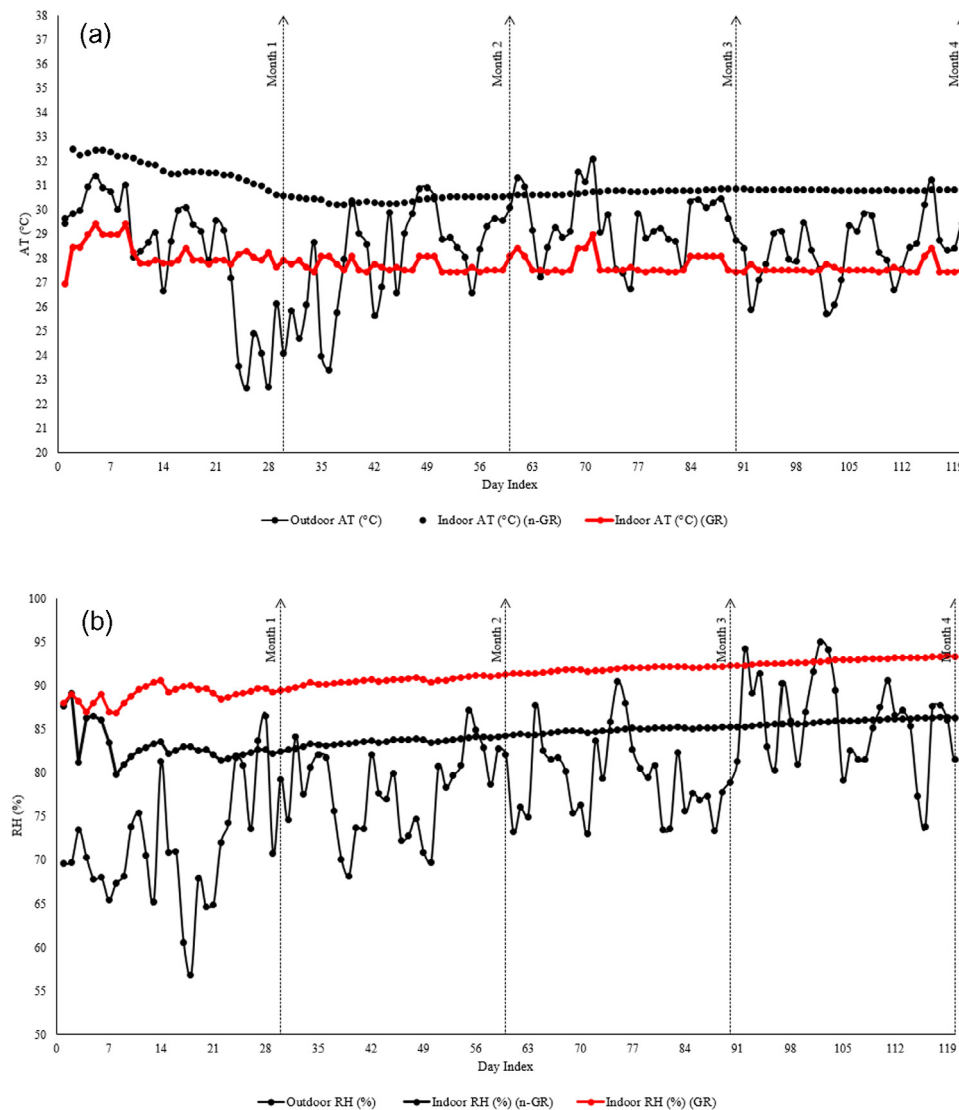


Fig. 4. (a) AT °C comparison of different months. Fig. 4. (b) RH % comparison of different months.

higher from 24% (n-GR) to 46% (GR) for the workers. For the month of June, risk level was higher (29%) and very high risk level was observed (26%) for n-GR condition which were transformed into moderate and lower risk condition due to GR construction. This indicates that GR had a better thermal insulation performance than n-GR (Fig. 7), although both roofs had the same slab thickness. This phenomenon may be caused by the difference of covering materials between the two roofs, in terms of their heat storage capacity, evaporative cooling and heat diffusion effects (Yang et al., 2015).

4.3. Indoor PHS prediction calculation

In this analysis, the heat stress criteria and environmental parameters were set for calculating indoor PHS (t_{sk} and t_{cr}) in accordance with previously established formula and computer generating program by Malchaire (2006) and Parsons (2006) which is based on ISO7933. For this predic-

tion (Table 5), the value of worker's (female) weight (53 kg), height (150 cm), body surface area (1.46 m²), Metabolic rate (116 W/m²), Clothing insulation (0.53 clo) have been considered to remain constant for the analysis. Here, female subjects have been considered for the evaluation because from the field monitoring, it has been identified that most of the workers in a garments factory are female (age 18–28 years) and they have various comfort perceptions depends on their different biological factors (Chowdhury et al., 2017). Most of them are involved in sewing activities which are indicated moderate activity (Met value 1.98). As a result, in this research constant subjective values have been used so that it could be accurately identified the indoor thermal conditions by using GR and n-GR through parametric studies.

4.3.1. Indoor t_{sk} prediction calculation

For the numerical and overall analysis of t_{sk} the internationally established formula has been implemented in

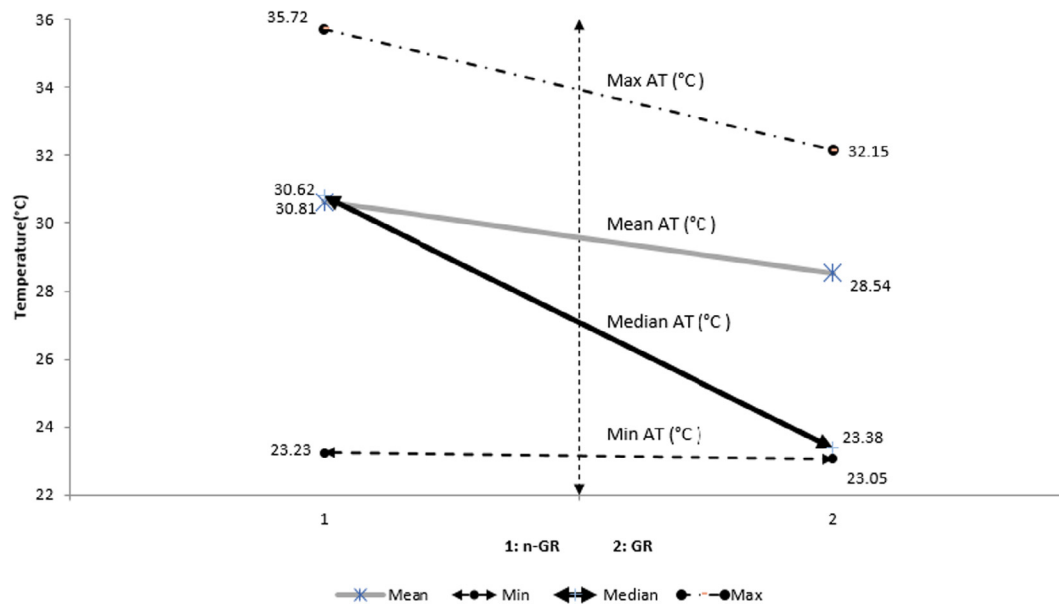


Fig. 5. Comparison of indoor thermal performance between n-GR and GR.

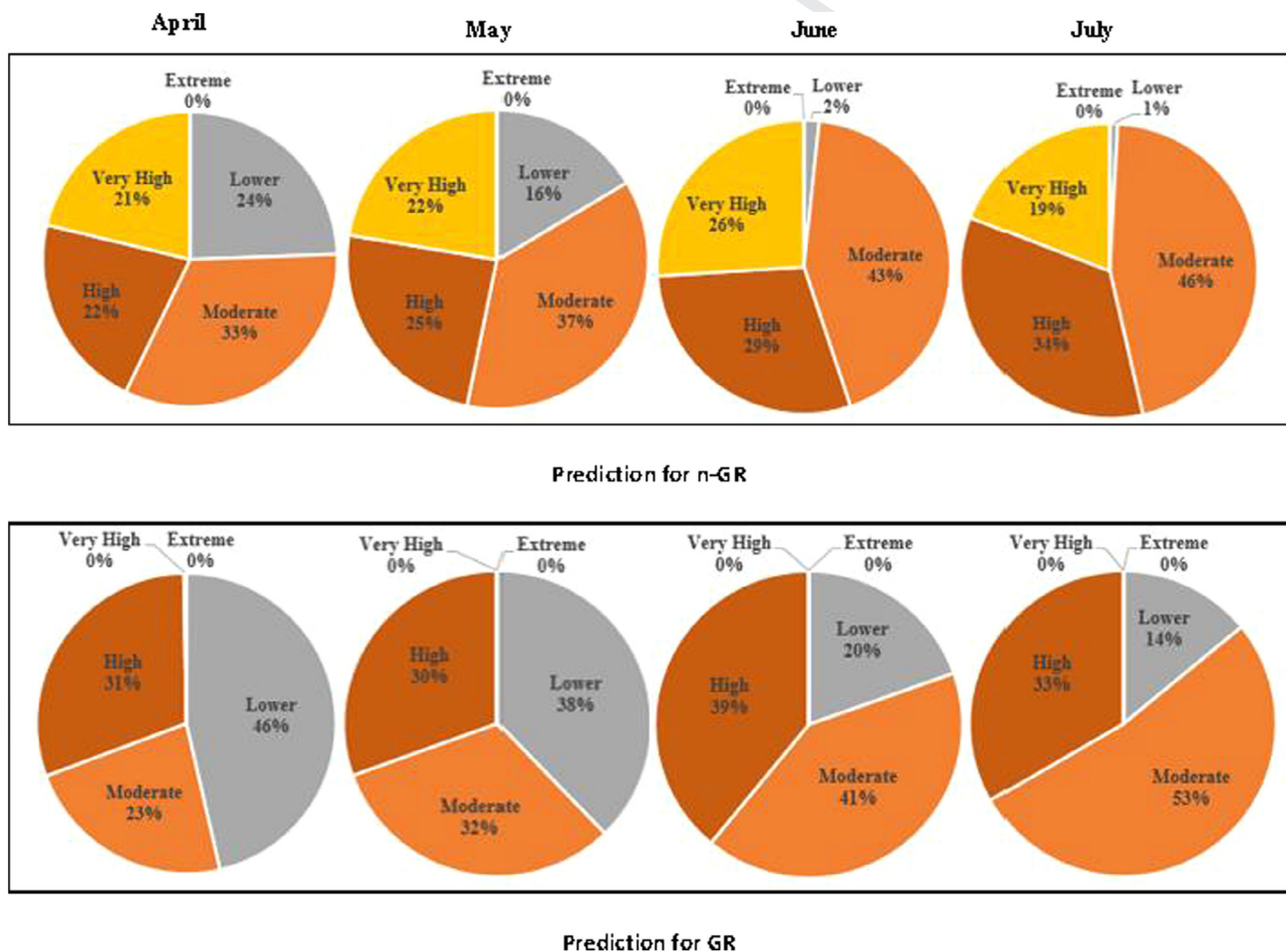


Fig. 6. Monthly WBGT (%) prediction and comparison for n-GR and GR construction.

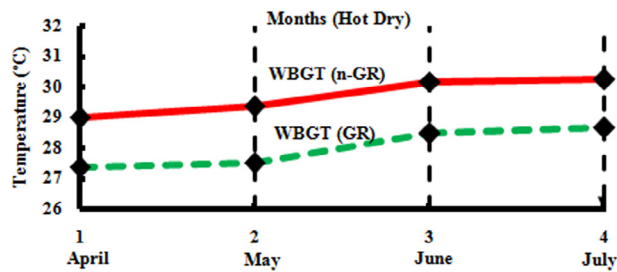


Fig. 7. Monthly average comparison of indoor WBGT for n-GR and GR construction.

accordance with ergonomics of the indoor thermal environment (Parsons, 2006; Lemke and Kjellstrom, 2012; Moran et al., 2001; Ergonomics of the thermal environment, 2004).

In this analysis, the following comfort condition has been considered for the prediction of indoor health risk phenomenon for the workers according to internationally established WBGT – PHS criteria (Table 6) (Chowdhury et al., 2017). Here, the considerations are as following: if

$t_{sk} \leq 24^\circ\text{C}$ indicates “Slightly Cool Uncomfortable”, if $t_{sk} \leq$ up to $24\text{--}26.5^\circ\text{C}$, indicates “Comfortable”, if $t_{sk} \leq$ up to $26.5\text{--}30^\circ\text{C}$, indicates “Slightly Warm”, if $t_{sk} \leq$ up to $30\text{--}35^\circ\text{C}$, indicates “Warm”, if $t_{sk} \leq$ up to $35\text{--}38^\circ\text{C}$, indicates “Hot” and if $t_{sk} >$ up to 38°C , “Very Hot” have been considered. From the above analysis (Fig. 8), it has been observed for the months of April–July t_{sk} level of the workers (n-GR) became almost 60% in hot condition and 35% in warm condition, where 4% indicates very hot level which might create short/long term constraint and for the extreme/very hot condition, it generates immediate constraint with health risk after 30–60 min of exposure which could be high health risk condition for the workers. In that case, average sweat rate of the workers has been indicated 220–360 g/h (Fig. 9) (Table 7). As a result for the month of April–July t_{sk} becomes higher than the normal body surface temperature (34.5°C). But for the GR construction type, indoor AT and WBGT becomes respectively lower and it reduces almost 25% higher discomfort level (Extreme, very hot and hot) without health risk for the factory workers. Although, in that case, for t_{sk} warm condition increases 20–23% more than n-GR condition which

Table 5
Worker's parameter for PHS studies.

Input	Unit	Value
Height	m	1.50
Body weight	kg	53
Adu (Body surface area)	m^2	1.46
Wind speed	m/s	0.20–0.25
Metabolic rate	met	1.98
External work	met	0.00
Icl (Clothes quantity)	clo	0.60
ter Rise of core temperature	C	0
tsk Rise of mean skin temperature	C	0
Actual measurement tsk	C	0.00
Measured weight loss density	g/hrm^2	0.00
Measured weight loss density	W m^{-2}	0.00
icl (Transparent sweat efficiency of clothes)		0.34
gcl,w (Moistness clothes thermal efficiency)		0.175
VO2 max% (oxygen uptake)	%	33–40 (60 Generation)
kadp (Perspiration coefficient)		1
Error t		0.001
Error t ₂		0.001
Wmax (skin wittedness)		0.85

[Here, metabolic rate (M) indicated moderate activity (sewing)].

Table 6
WBGT-PHS risk factor.

AT (°C)	Risk Factor	Metabolic Rate Limit (1 MET = 58.2 W/m ²)
≤ 26.6	Lower	Very High Activity $M > 260$
26.7 - 29.3	Moderate	Moderate to High Activity, $200 < M \leq 260$
29.4 - 31.0	Moderate to Risk	Moderate Activity $130 < M \leq 200$
31.1 - 32.1	Risk	Light Activity $65 < M \leq 130$
≥ 32.2	High Risk	Very Light Activity, $M \leq 65$

Source: ISO 7243 and the OSHA Technical Manual, Section III, Chapter IV, (Heat stress).

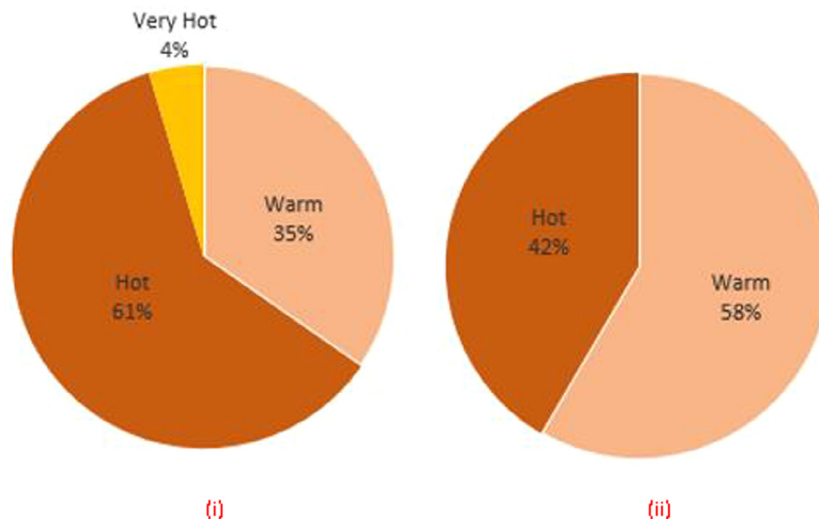


Fig. 8. Monthly average comparison of indoor t_{sk} for (i) n-GR and (ii) GR construction.

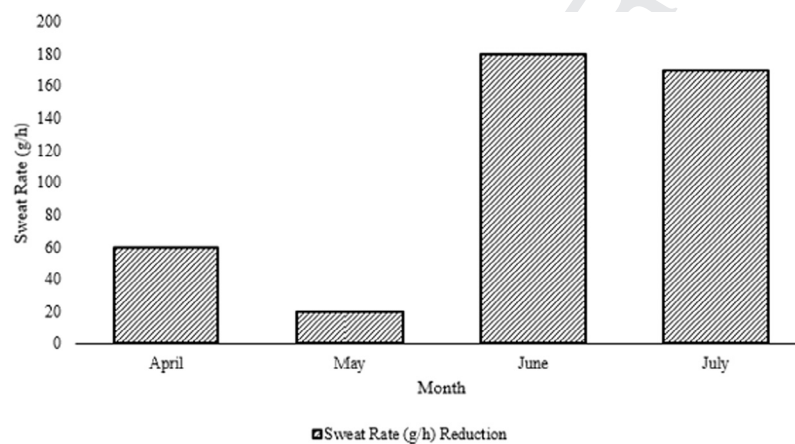


Fig. 9. Monthly average reduction of worker's sweat rate for GR implementation.

appears comfortable range with lower health risk for the workers (Fig. 8) according to the criteria.

4.3.2. Indoor t_{cr} prediction calculation

According to the prediction of t_{cr} (Parsons, 2006; Lemke and Kjellstrom, 2012; Moran et al., 2001; Ergonomics of the thermal environment, 2004; Parsons, 2009), long term or immediate constraint of health risk occurs even for a very extreme indoor thermal exposure (less than 30 min) (Table 6) for n-GR type. Therefore, a simple peripheral condition of the worker's body in PHS criteria was assumed for this analysis. In that case, t_{cr} becomes respectively higher than the limit (37.6 °C) due to the excessive indoor AT. Here, t_{cr} lines crossed the level of constant PHS temperature limit for the month of April–July and the maximum value has been examined almost upper than 38 °C (Fig. 10). This is because when the indoor AT exceeds body temperature, heat is taken from the environment. As soon as body temperature increases above the thermoregulatory set-point, it increases core temperature

(Chowdhury et al., 2017; Parsons, 2006; Lemke and Kjellstrom, 2012; Moran et al., 2001; Ergonomics of the thermal environment, 2004; Parsons, 2009). From the analysis, almost 30% high risk level and 56% upper limit condition than normal core temperature for the n-GR types, meanwhile, for the GR types was indicated, high risk level becomes almost zero (1%) and normal condition increases about 2.5 times higher than n-GR (Table 7) (Fig. 10). For this prediction the following criteria has been evaluated: if $t_{cr} \leq 37.6$ °C, indicates “Normal”, $t_{cr} \leq$ up to 37.6–38 °C, indicates “Upper Limit”, $t_{cr} >$ up to 38 °C, indicates “High Risk Level” according to the established formula of PHS (Moran et al., 2001; Ergonomics of the thermal environment, 2004; Parsons, 2009).

5. Cooling energy evaluation

To estimate the energy impact of the green roof, the total cooling energy (GJ) of the production space has been calculated for whole year with and without the green roof system.

Table 7

Monthly comfort comparison for n-GR and GR.

Month	Range	Interpretation (PMV-PPD)	PHS (n-GR)		PHS (GR)	
			Sweat Rate (g/h)	Risk Factor	Interpretation (PMV-PPD)	Sweat Rate (g/h)
	Min.	Cold	100	No Health Risk	Cold	60
April	Avg.	Very Hot	220	Discomfort Without health Risk	Hot	180
	Max.	Extreme Hot	360	Immediate Constraint	Very Hot	340
	Min.	Comfortable	70	No Health Risk	Cold	60
May	Avg.	Hot	190	Discomfort Without health Risk	Hot	180
	Max.	Very Hot	330	Short-term Constraint	Very Hot	320
	Min.	Hot	120	Comfort: No Health Risk	Comfortable	110
June	Avg.	Very Hot	250	Discomfort Without health Risk	Hot	70
	Max.	Extreme Hot	350	Immediate Constraint	Very Hot	220
	Min.	Hot	120	Comfort: No Health Risk	Cold	20
July	Avg.	Very Hot	230	Discomfort Without health Risk	Comfortable	60
	Max.	Very Hot	330	Short-term Constraint	Very Hot	160

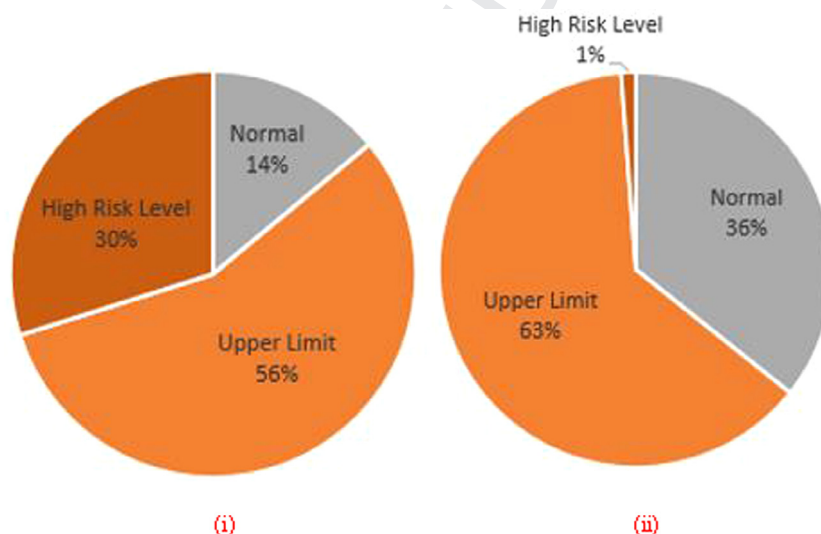
SD, AT (°C) = ± 1 °C and SD, RH (%) = ± 5 %.Fig. 10. Monthly average comparison of indoor t_{cr} for (i) n-GR and (ii) GR construction.

Fig. 11(a) and (b) provide the annual cooling energy reduction for the production space, which is a zone that is seriously affected by the presence of the green roof system. As shown, the GR reduces the secondary cooling energy (electricity) of the whole building from 46 to 50 GJ, which is equivalent to a reduction close to 153 GJ primary energy (electricity) systems with the conversion factor (Site > Source, which are the multipliers to convert Site energy into Source energy for electricity) 3.34 ratio from secondary to primary energy. As a result, the annual total cooling energy

of the production space is reduced from 350 GJ to 298 GJ, a reduction close to 13% (primary energy) by using GR techniques. It has been noted here that the percentage of the achieved energy conservation is a strong function of the zone and building size, orientation, shape, envelope, its structural characteristics and also of the indoor operational thermal conditions and scheduling. Finally, it was also observed from this analysis, direct contact with the GR of the upper floor contributes to energy reduction of its annual cooling demand for that particular building.

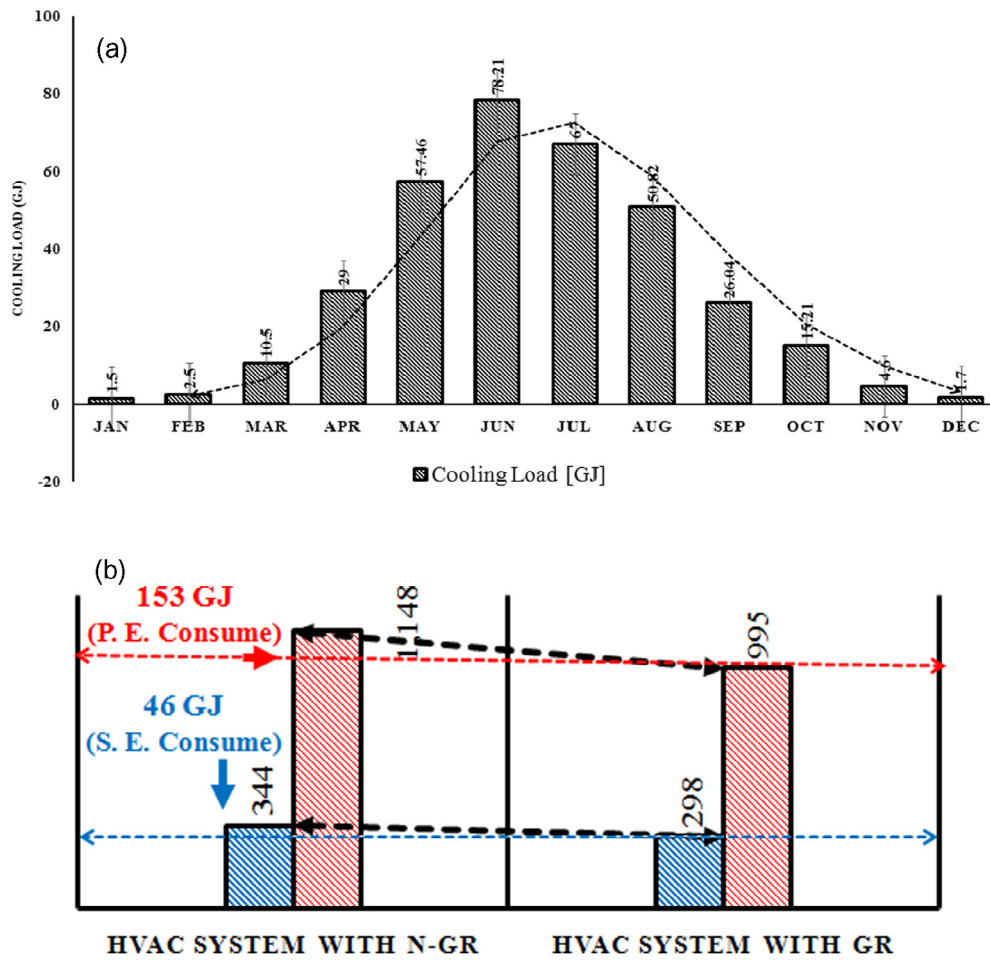
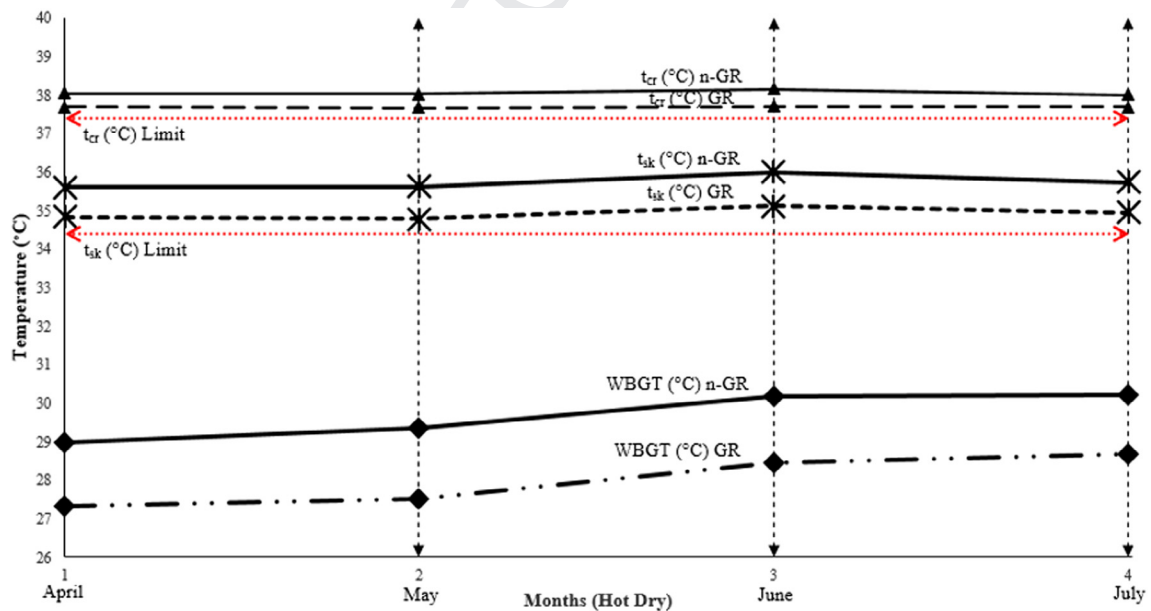


Fig. 11. (a) Monthly cooling demand Fig. 11 (b) Energy reduction by using GR system.

Fig. 12. Monthly overall comparison of worker's WBGT, t_{sk} and t_{cr} for n-GR and GR implementation.

6. Study limitations

The basic research methodology of this particular study draws on from previous research undertaken by the authors (Chowdhury et al., 2015). The methodology and samples did not allow us to implement all diversities into numerical models for simulations. Some characteristics of the production space including numerous variables and design parameters which were not all captured, outdoor air quality, surface heat transfer coefficient, insulation, human thermal physical factors (Buchin et al., 2015b; Chowdhury et al., 2017) and pollutants, all of which may impact the concentrations of indoor thermal environment, were not main focus of this analysis (Mahmoud et al., 2017; LiW and YeungK, 2014; Peng and Jim, 2013).

7. Conclusions

The most major observations of this study is that WBGT and PHS criteria (Table 6) for the labor intensive factory are not stagnant and varies for the change of local construction types. It has been concluded and correlated from the above result analyses that (Fig. 12):

- The GR condition has the bigger temperature attenuation, meanwhile, the n-GR presented the worse thermal insulation performance compared to GR.
- The zone with the GR at summer operation could create a much cool indoor AT that is 2.5–3.5 °C lower than n-GR construction type.
- According to annual physiological comfort criteria (Chowdhury et al., 2015; Shabbir Ahmed, 2003; Parsons, 2006; Lemke and Kjellstrom, 2012), about 45% indoor environment appears hot (danger level) of the factory workers for n-GR and rest 35% indicates warm condition which may occur serious health risks of heat stroke.
- According to the measured and predicted Values, WBGT, t_{sk} and t_{cr} of factory workers for both n-GR and GR have significant indoor heat stress impact during peak working condition (12.00–3.00 pm) due to zone heat fluctuation.
- For the summer condition (April–July) in Dhaka, Bangladesh, PHS criteria appears at very high risk level (WBGT 45%, t_{sk} 30–55% and t_{cr} 50–65%) with short/long and immediate constraint for n-GR construction which can be reduced almost 2–2.5 times with GR construction.

This indicated that GR could reduce the indoor heat stress, thus creating a better thermal comfort environment. In this study, concentrations of local n-GR and GR have been measured with the parametric studies. Some characteristics like insulations, HVAC system, energy consumption, GR layering, LAI and pollutants, all of which may affect the concentrations of indoor thermal environment and health risk reduction of workers which will be needed

for further detail analysis. Finally, the guidelines suggested in this study will help designers while designing an energy efficient labor intensive factory production space with accommodating compliances in the tropics.

Uncited references

Coma et al. (2014), Li et al. (2010), and Lin et al. (2013).

Acknowledgments

Appreciation goes to the Green Architecture Cell (GrACe), (Dept. of Architecture), BUET, Bangladesh, GIZ, Dhaka, Bangladesh, Environmental Lab, (Dept. of Architecture), CUET, Bangladesh and specially Laboratory of Environmental Ergonomics (Human Environmental System), Hokkaido University, Japan. The authors would like to specially thank Dr. Srabanti Karmakar (Medical Doctor, Bangladesh) and Maria Fernanda Rivas (Climate Change) who have provided assistances in numerous ways.

References

- Al-Zubaydi, Ahmed Y., 2013. Building models design and energy simulation with google sketchup and open studio. *J. Adv. Sci. Eng. Res.* 3 (4), 318–333.
- Bangladesh Garment Manufacturers and Exporters Association (BGMEA), 2015. Available at: <http://www.bgmea.com.bd/> [accessed 08.12.2015].
- Bernard, Thomas E., Mark Hanna, W., 1988. Environmental effects on WBGT and HSI using a computer simulation. *Int. J. Ind. Ergon.* 3, 103–113.
- Buchin, Oliver. et al., 2015a. Evaluation of the health-risk reduction potential of counter measures to urban heat islands. *Energy Build.*
- Buchin, Oliver et al., 2015b. Evaluation of the health-risk reduction potential of countermeasures to urban heat islands. *Energy Build.*
- Chowdhury, Sajal, Alam, Md. R., 2011. Design approach of energy efficient ready-made garments factory in view of thermal comfort, Republic of Korea Published by IAARC, s1–s3, pp. 27–32.
- Chowdhury, Sajal, Shabbir Ahmed, Khandaker, Hamadaa, Yasuhiro, 2015. Thermal performance of building envelope of ready-made garments factories in Dhaka, Bangladesh. *Energy Build.* 107 (15), 144–154.
- Chowdhury, Sajal, Hamada, Yasuhiro, Shabbir Ahmed, Khandaker, 2017. Experimental evaluation of subjective thermal perceptions for sewing activity. *Energy Build.* 149 (15), 450–462.
- Chowdhury, Sajal, Chowdhury, Sajal, Hamada, Yasuhiro, Shabbir Ahmed, Khandaker, 2017. Prediction and comparison of monthly indoor heat stress (WBGT and PHS) for RMG production spaces in Dhaka, Bangladesh. *Sustainable Cities Soc.* 29, 41–57.
- Coma, Julia et al., 2014. New green facades as passive systems for energy savings on buildings. *Energy Procedia* 57, 1851–1859.
- Crawley, Drury B. et al., 2001. Energy Plus: creating a new-generation building energy simulation program. *Energy Build.* 33 (4), 319–331.
- EnergyPlus, 2015. U.S. Department of Energy, USA.gov. Dhaka419230 (SWERA), Weather Data, 2014, EnergyPlus, U.S. Department of Energy, USA.gov. Available-at: <http://apps1.eere.energy.gov/buildings/energyplus/cfm/weather_data3.cfm/region=2_asia_wmo_region_2/country=BGD/cname=Bangladesh> (accessed 04.08.2015).
- Ergonomics of the thermal environment – Analytical determination and interpretation of heat stress using calculation of the predicted heat strain, ISO/FDIS 7933:2004.

- Fiorito, Francesco, 2014. Phase-change materials for indoor comfort improvement in lightweight buildings. A parametric analysis for Australian climates. *Energy Procedia* 57, 2014–2022.
- Hygh, Janelle S. et al., 2012. Multivariate regression as an energy assessment tool in early building design. *Build. Environ.* 57 (11), 165–175.
- Lemke, Bruno, Kjellstrom, Tord, 2012. Calculating workplace WBGT from meteorological data: a tool for climate change assessment. *Ind. Health* 50, 267–278.
- Li, Ji-feng et al., 2010. Effect of green roof on ambient CO₂ concentration. *Build. Environ.* 45 (12), 2644–2651.
- Lin, Bau-Show et al., 2013. Impact of climatic conditions on the thermal effectiveness of an extensive green roof. *Build. Environ.* 67, 26–33.
- LiW, C., YeungK, K.A., 2014. A comprehensive study of green roof performance from environmental perspective. *Int. J. Sustainable Built Environ.* 3 (1), 127–134.
- Mahmoud, Abubakar S. et al., 2017. Energy and economic evaluation of green roofs for residential buildings in hot-humid climates. *Buildings* 7 (2), 30. <https://doi.org/10.3390/buildings7020030>.
- Malchaire, J.B.M., 2006. Occupational heat stress Assessment by the Predicted Heat Strain model. *Ind. Health* 44, 380–387.
- Bangladesh Meteorological Department, 2015. IDB Bhaban, Begum Rokeya Sarani, Dhaka 1207, Bangladesh. (www.bmd.gov.bd) (accessed 07.07.2015).
- Moran, D.S. et al., 2001. An environmental stress index (ESI) as a substitute for the wet bulb globe temperature (WBGT). *J. Therm. Biol.* 26 (4–5), 427–431.
- Nahar et al., 2010. Occupational health hazardous in garment sector. *Int. J. Biomed. Res.* 1 (2), 01–06.
- Naz, Farah, 2008. Energy Efficient garment factories in Bangladesh. PLEA 2008–25th Conference on Passive and Low Energy Architecture, Dublin, 22nd to 24th October.
- Parsons, K., 2006. Heat stress standard ISO 7243 and its global application. *Ind. Health* 44 (3), 368–379.
- Parsons, K.C., 2009. Maintaining health comfort and productivity in heat waves. *J. Global Health Action* 2, 39–45. <https://doi.org/10.3402/gha.v2i0.2057>, ISSN 1654-9880.
- Peng, Lilliana L., Jim, C.Y., 2013. Green-roof effects on neighborhood microclimate and human thermal sensation. *Energies* 6, 598–618. <https://doi.org/10.3390/en6020598>.
- Shabbir Ahmed, Khandaker, 2003. Comfort in urban spaces: defining the boundaries of outdoor thermal comfort for the tropical urban environments. *Energy Build.* 35 (1), 103–110.
- Wittwer, J.W., 2004. “Graphing a Normal Distribution in Excel”. From Vertex42.com, November 1, 2004 <http://www.vertex42.com/ExcelArticles/mc/NormalDistribution-Excel.html>.
- Yang, Wansheng et al., 2015. Comparative study of the thermal performance of the novel green (planting) roofs against other existing roofs. *Sustainable Cities Soc.* 16, 1–12.